Application of Hydrological Model Simulations in Landslide Predictions

Binru Zhao[1,2], Qiang Dai[3], Dawei Han[2], Jun Zhang[2], Lu Zhuo[2,4], and Matteo Berti[5]

[1] College of Water Conservancy and Hydropower Engineering, Hohai University, Nanjing, China.

[2] Department of Civil Engineering, University of Bristol, Bristol, UK.

[3] Key Laboratory of VGE of Ministry of Education, Nanjing Normal University, Nanjing, China.

[4] Department of Civil and Structural Engineering, University of Sheffield, Sheffield, UK.

[5] Dipartimento di Scienze della Terra e Geologico-Ambientali, Università di Bologna, Bologna, Italy.

Corresponding author: Qiang Dai (e-mail: bz17336@bristol.ac.uk, Tel: 447410376012)

Acknowledgments

The authors acknowledge the Emilia-Romagna Geological Survey for providing landslides data and Arpae Emilia-Romagna organization for providing the meteorological data and flow data. The authors also acknowledge Dr. Stephen Birkinshaw from the University of Newcastle for the help with SHETRAN in this study. The first author would like to thank the China Scholarship Council for funding her study at the University of Bristol. This study is supported by Resilient Economy and Society by Integrated SysTems modelling (RESIST) (Newton Fund via Natural Environment Research Council (NERC) and Economic and Social Research Council (ESRC) (NE/N012143/1)), National Natural Science Foundation of China (41871299) and the Fundamental Research Funds for the Central Universities of China (2016B42014).

Abstract

The importance of soil moisture conditions in the initiation of landslides has been widely recognized. This study takes advantage of the distributed hydrological model to derive the soil wetness index. The derived soil wetness index is then used to determine soil wetness thresholds for landslide occurrences. In order to predict landslides based on alert zones, a zone threshold is introduced together with the soil wetness threshold to constitute the integrated threshold. We evaluate the prediction performance of the integrated thresholds with the use of skill scores and the receiver operating characteristic (ROC) curves. This study is carried out in a sub-region of the Emilia-Romagna region, Northern Italy. Results show that the derived soil wetness index could account for the hydrological process that is controlled by meteorological conditions and topographic properties. The proposed integrated threshold shows a better predictive capability than the rainfall threshold, demonstrating the effectiveness of applying the soil wetness index in landslide predictions. The optimal threshold is also determined by compromising the correct predictions and incorrect predictions, it is found that the optimal integrated threshold is more advantageous in reducing false alarms compared with the optimal rainfall threshold. This study highlights the potential of applying hydrological simulations in landslide prediction studies and provides a new way to make use of high-resolution data in zone-based landslide predictions.

Keywords

Hydrological simulation; Soil wetness index; Landslide threshold

1 Introduction

Landslide is one of the most frequent and widespread natural disasters, with a significant threat to human lives and properties. Although the occurrence of landslides could be a result of multiple factors, such as earthquakes, volcanoes, floods, and heavy rainfall, rainfall is the most common trigger of slope failures. Predicting the occurrence of rainfall-induced landslides is of both scientific importance and practical needs, playing an important role in mitigating the impact of landslides.

Rainfall thresholds are the main conventional tools to study the relationship between rainfall and landslide occurrences, which are defined as the minimal rainfall conditions that are likely to trigger landslides on the basis of empirical observation (Guzzetti et al. 2007). The critical rainfall conditions are characterized by different indicators, like cumulated event rainfall (Cardinali et al. 2006), rainfall duration (Gariano et al. 2015, Peruccacci et al. 2012), rainfall intensity and the combination of rainfall intensity and duration. Among these indicators, the rainfall intensity-duration (ID) is more widely used (Dahal and Hasegawa 2008, Guzzetti et al.

2007, Guzzetti, et al. 2007). However, only considering rainfall intensity or/and duration information is not sufficient to assess the landslide threat, because the antecedent soil moisture conditions also play a crucial role in landslide occurrences (Baum and Godt 2009, Campbell 1975, Segoni et al. 2009).

Although the importance of soil moisture conditions in the initiation of landslides has been widely recognized, the direct use of soil moisture information in landslide studies is still largely unexplored. Most studies use antecedent precipitation indices as a proxy for soil moisture (Crozier 1999, Glade et al. 2000, Zêzere et al. 2015, Zhao et al. 2019). The length of antecedent periods is difficult to determine, which varies widely in published literature, e.g., from a few days (Calvello et al. 2015) to a few months (Zêzere et al. 2005). Additionally, some studies have found that the antecedent precipitation is not well correlated with the actual soil moisture condition, and it is not recommended to use the antecedent precipitation as the proxy of soil moisture (Baum and Godt 2009, Brocca et al. 2008).

Several researchers (e.g., Brocca et al. (2012), Mirus et al. (2018), Zhuo et al. (2019)) have more explicitly included soil moisture information in landslide predictions. A few studies take advantage of remotely sensed soil moisture data. For example, Brocca, et al. (2012) used the ASCAT-derived soil moisture data in landslide forecasting. Ray et al. (2010) used downscaled AMSR-E soil moisture in landslide susceptibility mapping. Zhuo, et al. (2019) proposed soil moisture thresholds for landslides under different environmental conditions (land cover, soil type and slope), with the use of remotely sensed soil moisture. Although these studies demonstrate the effectiveness of using satellite soil moisture in landslide researches, the remote sensed soil moisture suffers from a coarse resolution in both time and space and large estimation uncertainties (Temimi et al. 2010), limiting its use in landslide studies. In-situ measurement is another way to obtain soil moisture information. The data from in-situ measurements is more accurate on individual points. Considering the spatial variations of soil moisture in landslide-prone areas, a dense measurement network is needed to provide the required spatial information. However, due to the high cost of the installation and maintenance, dense soil moisture sensors are not practically feasible. Therefore, the scarcity of reliable in-situ soil moisture measurement hampers its application in practice. Only a few studies explore its use in landslide researches (Baum and Godt 2009, Greco et al. 2010, Hawke and McConchie 2011, Mirus, et al. 2018). The model-based method is an alternative for soil moisture estimation, like the land surface model and the hydrological model. The ability of hydrological simulations in providing vital information for landslide hazards has been examined by some recent studies (Posner and Georgakakos 2015, Valenzuela et al. 2017, Zhao et al. 2019). However, there is still a large knowledge gap in such researches which needs to be filled (e.g., how to derive soil moisture information from the distributed hydrological model, and how to make full use of high-resolution data in landslide predictions).

The objective of this study is to further explore the application of hydrological simulations in landslide predictions. Specifically, a distributed hydrological model is used to derive the soil wetness index, which could account for both the meteorological conditions and the topographic properties. The derived soil wetness index together with landslide data are then used to establish integrated thresholds for landslide occurrence. We evaluated the prediction performance of the proposed thresholds using different skill scores and the receiver operating characteristic (ROC) curves. A sub-region of the Emilia-Romagna Region in Northern Italy is chosen as the study area considering the landslide susceptibility and data availability. The study period is chosen from 2005 to 2015, because during this period all the required data are recorded adequately. The data of the first eight years (as the calibration period from 2005 to 2013) are used to define the thresholds for landslide occurrences, while the data of the last two years (as the validation period from 2014 to 2015) are for the evaluation of the derived thresholds.

This paper is organized as follows. Section 2 introduces the study area and sources of data. Section 3 details the hydrological model, methods of determining landslide thresholds and procedures of thresholds evaluation. Results are analyzed in Section 4, followed by further discussions in Section 5. Conclusions and outlook are summarized in the final section.

2 Study Area and Data

2.1 Study Area

The Emilia-Romagna region is located in the north of Italy. Its northern and eastern portions are a wide flat area, while the southern and western portions are mountainous areas, whose maximum altitude reaches 2165 m (Figure 1). The region has a typical Mediterranean climate with warm and dry summers and mild/cold wet winters.

The mountainous area of the region belongs to the northern Apennines chain and covers around 12,000 km^2. The Apennines chain is a thrust and fold belt with a very complex setting, which formed due to the collision between the European plate and the Adria microplate and the closing of the ocean called Tethys (Vai et al. 2001). The bedrock geology of this area is characterized by clastic rocks, flysch and clays units (Bettelli and Vannucchi 2003, Pini 1999). The complex geological setting controls the local morphology and the abundance of landslides, with more than 20% of the mountainous area covered by active or dominant landslide deposits (Berti et al. 2012). The landside type is also various, with slow earth flows, rotational-translational slides and complex movements being the most frequent (Bertolini and Pellegrini 2001). In general, rainfall is the main triggering factor of landslides in this region. Shorter but extraordinarily intense rainfalls are likely to trigger debris flows and shallow landslides, while moderate but extraordinarily prolonged periods of rainfalls lead to earthflows and deep-seated landslides (Ibsen and Casagli 2004). Although landslides do not usually result in causalities, they may cause

significant damages to properties and infrastructures. The cost of regeneration and remedial works have approximately been €130 million during the period of 2008 to 2012 (Berti, et al. 2012). With the recent developments in the mountainous area and the increase of the distributed population, the damage and cost will be more significant.

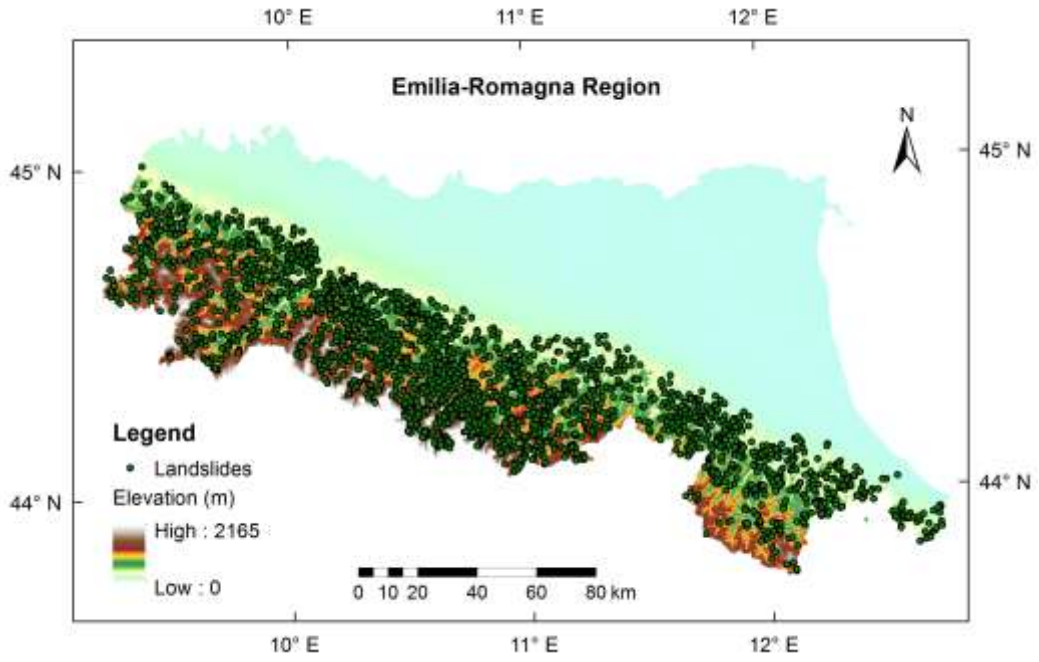

Figure 1. Map of the Emilia-Romagna region and landslides in this region.

Two catchments in the mountainous area are chosen as the study area due to the availability of the hydrometeorological data and landslide records (Figure 2). These two catchments are mainly covered by trees and crops, and characterized by a terrain ranging from hilly and mountainous sectors in the S-SW to wide plain towards NE, with the altitude varying from 8 m to 2153 m. Catchment 1 has an area of 1191 km^2, and Catchment 2 of 722 km^2. The flow monitoring stations at the outlet of these two catchments provide daily flow data for the period from 2004 to 2015. There are 11 weather stations operated within Catchment 1, and 5 within Catchment 2, providing data of precipitation, air temperature and mean wind speed at a daily resolution for the same period. During the study period from 2005 to 2015, 130 and 144 landslides are recorded for Catchment 1 and Catchment 2, respectively.

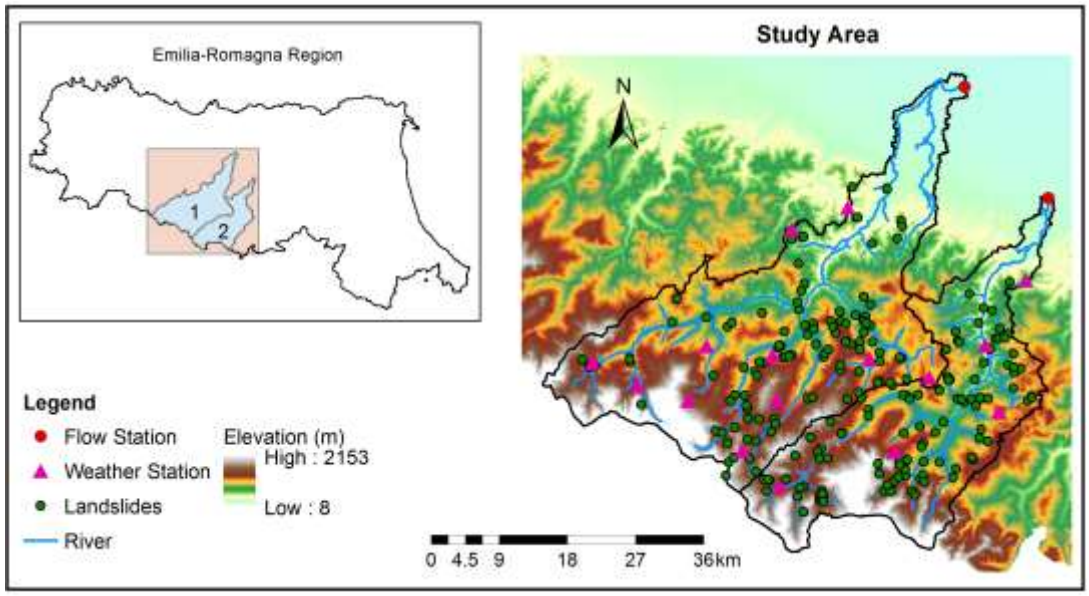

Figure 2. Map of the study area with the terrain elevation and the distribution of weather stations, flow stations and landslides.

2.2 Landslide Database

The adopted landslide information is from the Emilia-Romagna Geological Survey, an agency maintaining a catalog of historical landslides in the Emilia-Romagna region. The catalog collects landslide information from various sources, such as reports to local authorities, national and local press, technical documents. Although this catalog is not very complete for all landslides, especially those occurred in remote areas with minor phenomena, it contains most landslides causing some sort of damage. This catalog is statistically more detailed since around 1951, considered as a proxy of actual landslides (Rossi et al. 2010). For each landslide, the catalog records the information of its location, date of occurrence, date accuracy, landslide characteristics (length, width, type and material), triggering factors, damage and references. Unfortunately, not all information is available for all landslides, and in most cases, only the location and occurrence date are recorded.

Based on the available information, rainfall-induced landslides in the study area are selected for analysis. There is a total of 274 landslides over the study period 2005-2015, among which 235 landslides occurred during the calibration period from 2005 to 2013, with the rest for the validation period from 2014 to 2015. The selected landslides are mapped as dots in Figure 2, with some dots overlapping.

2.3 Rainfall Database

The 16 weather stations distributed in the study area have tipping-bucket rain gauges, being able to collect rainfall data at a daily time scale before 2001 and every 30 minutes since 2001.

Although a high resolution of rainfall data is available over the study period, most of the other required data are at a daily resolution, which restricted the time resolution of this study to be daily. The rainfall database is accessed online (http://www.smr.arpa.emr.it/dext3r/), carried out by the Regional Agency for the Prevention, Environment and Energy of Emilia-Romagna (Arpae).

2.4 Other Datasets

In addition to the landslide catalog and rainfall database, other datasets are needed to support the hydrological simulations. Meteorological data (like rainfall, air temperature and wind speed) are required to force the hydrological model, and the flow data are used to calibrate the model. Besides, environment features (i.e., DEM, land cover and soil type) are necessary to characterize the studied catchment for hydrological simulations. The measurements of meteorological and flow data are carried out by the Regional Agency for the Prevention, Environment and Energy of Emilia-Romagna (Arpae) (http://www.smr.arpa.emr.it/dext3r/). Land cover information is extracted from the ESA CCI land cover map (v2.0.7) and the soil type information is from the SoilGrids-World Reference Base class (TAXNWRB). As for the DEM data, we use the Shuttle Radar Topography Mission (SRTM) 3 Arc-Second Global DEM datasets (90m).

3 Methodology

3.1 Definition of rainfall events and rainfall thresholds

The first step in the definition of rainfall thresholds is to identify the rainfall events that have triggered landslides and those without landslides, described by its duration (D) and cumulated event rainfall (E). In order to make the definition of rainfall events objective and reproducible, the automatic procedure proposed by Melillo et al. (2014) is applied to reconstruct rainfall events for the daily rainfall measurements from each rain gauge. Additionally, this procedure is capable of identifying the rainfall conditions that are likely to result in landslides and calculating their duration (D) and cumulated event rainfall (E). The algorithm requires an input parameter to define the minimum dry period between two consecutive rainfall periods, and this parameter can vary with seasonal and climatic conditions. Given the Mediterranean climate of the study area, we set a dry period of 4 days for the cold season, and 2 days for the warm season. The cold season and warm season are classified based on a function of the climate and altitude, as the work of Peruccacci et al. (2017), where the cold season is from October to April and the warm season is from June to September.

The empirical rainfall thresholds are then determined with all the possible rainfall conditions responsible for landslides. In this study, we adopted the Frequentist approach proposed

by Brunetti et al. (2010). The general form of threshold curves is a power law linking the cumulated event rainfall E (mm) to the rainfall duration D (day):

$$E = \alpha \cdot D^{\gamma} \quad (1)$$

where α is a scaling constant (the intercept), γ is the shape parameter (that defines the slope of the power law curve). In this study, the rainfall thresholds with 12 different exceedance probabilities (from 1% to 50%) are calculated and explored.

When applying the derived rainfall threshold in landslide predictions, alert zones (AZs) are used for hydrometeorological monitoring and early warning. The alert zones are classified according to the location of weather stations using the method of Thiessen polygons (Croley II and Hartmann 1985). When the rainfall event in an alert zone exceeds the rainfall threshold, the landslide occurrence is predicted, otherwise, the landslide non-occurrence is predicted. Figure 3a and Figure 3b give an illustration of the procedure. This zone-based prediction scheme is recommended by Gariano, et al. (2015), because it could consider the inherent lack of landslide information compared with the prediction scheme based on rain gauges.

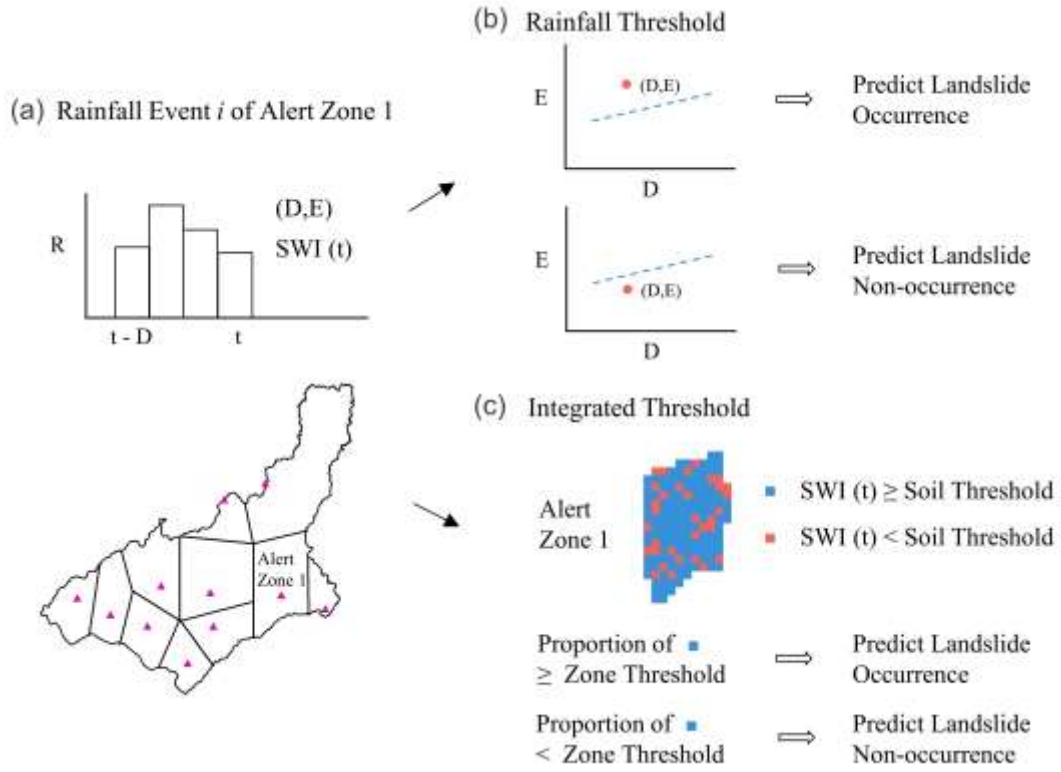

Figure 3. The illustration of the prediction scheme for rainfall threshold and integrated threshold.

3.2 Hydrological model SHETRAN

Système Hydrologique Européen TRANsport (SHETRAN) is a distributed hydrological model, designed for the simulation of basic processes and pathways for flow and transport in river catchments (Ewen 1995). It is originated from the Système Hydrologique Européen (SHE) (Abbott et al. 1986). The model has been applied in a wide range of catchments and proved to be a reliable hydrological model (Birkinshaw 2008, Birkinshaw and Ewen 2000, Norouzi Banis et al. 2004, Zhang and Han 2017, Zhang et al. 2013). As SHETRAN is based on physical processes and spatially distributed, it is considered effective to simulate soil moisture evolution in response to rainfall conditions at a grid scale.

Table 1 Equations of Hydrological Processes in SHETRAN

Processes	Equation
Evaporation	Penman-Monteith equation (or a fraction of potential evaporation rate) (Abbott, et al. 1986)
Canopy interception and drip	Rutter equation (Abbott, et al. 1986)
Subsurface flow	Variably saturated flow equation (3D) (Parkin 1996)
Overland flow	Saint-Venant equations, diffusion wave approximation (2D) (Abbott, et al. 1986)
Channel flow	Saint-Venant equations, diffusion wave approximation (flow in a network of 1D channels) (Abbott, et al. 1986)
Snowpack and melt	Accumulation equation and energy budget melt equation (or degree-day melt equation) (Abbott, et al. 1986)

SHETRAN has three main components: water flow, sediment transport and contaminant transport. Water flow component contains major elements of the hydrological cycle, as shown in Table 1. Net precipitation is calculated from incoming precipitation with the extraction of interception and evapotranspiration. The actual evapotranspiration rates are calculated as a function of dynamic soil moisture conditions. Surface water is produced by infiltration excess or saturation excess mechanisms, and it is routed into a channel as overland flow. Both the overland and channel phases are calculated on the basis of the diffusive wave approximation of the full Saint-Venant equations, which allows backwater effects to be modelled (Abbott, et al. 1986). Infiltration into the ground is from net precipitation and surface water. For unsaturated zone, soil moisture content and tension are calculated; for saturated zone flows, they are computed for a heterogeneous, anisotropic, unconfined aquifer using variably saturated flow equation (3D) (Parkin 1996). Exchange flows which occur between the aquifer and a partly penetrating channel are also calculated in this model. The parameters used in this model are listed in Table 2.

Meteorological inputs to SHETRAN include precipitation and potential evapotranspiration (measured or calculated). In this model, the physics-based governing partial differential equations

for flow and transport are solved on a three-dimensional grid, which can take into account the spatial variation of the meteorological information and catchment properties. However, in this study, only the DEM property and meteorological inputs are spatially distributed. The spatial distribution of meteorological inputs is based on Thiessen polygons, which is set up according to the location of weather stations. The rainfall and evapotranspiration conditions are assumed to be the same in the polygon, provided by its weather station. The land cover and soil type information are assumed uniform. There are two reasons for this setting. First, according to the land cover and soil type information of the study area, it is found most areas are characterized by similar information. Most areas are covered by tree and crop and the main soil type is gleyic solonetz. Second, due to the lack of field measurements of properties of the soil and land cover, model parameters related to these properties need to be calibrated. As a result, considering the spatial variation of the soil type and land cover will result in too many parameters, causing problems like over-fitting. Therefore, in order to keep the balance between the model efficiency and accuracy, we adopt the uniform information on soil type and land cover, in this way, the model simulations rely on spatially uniform parameters. This simplification of the model setting raises a question: the simulated soil moisture is not the 'true' soil water content. It can only be regarded as an index to indicate the soil wetness condition. The simulated soil moisture has different variation ranges for different grid cells, due to the impact of topography. In order to make the soil wetness conditions comparable, the simulated soil moisture is scaled based on the soil moisture variation range of its grid cell. The scaled value is referred as Soil Wetness Index (SWI). The superiority of the derived index is that it is not only able to account for the rainfall and evapotranspiration conditions, but also take into consideration the impact of topography on the hydrological process.

Table 2 Parameters Used in the Hydrological Model SHETRAN

Vegetation	Canopy storage capacity (mm)
	Leaf area index
	Maximum rooting depth (m)
Soil properties	Saturated water content
	Residual water content
	Saturated conductivity (m/day)
	Van genuchten-alpha (cm^{-1})
	Van genuchten-n
	Soil depth (m)
Others	AE/PE ratio at field capacity
	Strickler overland flow roughness coefficient ($m^{1/3}$ s^{-1})

The model parameters are calibrated with the observed flow data at the outlet of the catchment. Nash-Sutcliffe efficiency (NSE) (Nash and Sutcliffe 1970) is used to minimize the difference between the observed and simulated flow. The model is calibrated with the data of the period 2004-2013, with the first year as the warm-up period, and then validated for the period 2014-2015. The spatial resolution of our model is 1 km, which is a compromise between model performance and computational efficiency.

3.3 Definition of integrated thresholds

The soil wetness threshold is determined by analyzing the soil wetness index of the landslides during the calibration period, which is defined as the soil wetness conditions that when reached or exceeded, are likely to trigger landslides.

The soil wetness index derived from the hydrological model is at a grid scale, however, it is not feasible to predict landslides at a grid scale in practice. Considering the operability in landslide predictions and the comparability with the rainfall threshold, a zone threshold is introduced. A combination of soil wetness threshold and zone threshold is used to predict landslides, referred as the integrated threshold. The prediction scheme of the integrated threshold is illustrated in Figure 3a and Figure 3c. For a rainfall event in an alert zone, the soil wetness index of the last day of the rainfall event is estimated for each grid in the zone. Each soil wetness index is then compared with the soil wetness threshold, if the soil wetness index exceeds the threshold, its grid cell is marked as the wet grid cell. The zone threshold is then used to evaluate the proportion of wet grid cells in an alert zone. If the proportion of wet grid cells exceeds the zone threshold, landslide occurrence is predicted, otherwise, landslide non-occurrence is predicted. In this study, various combinations of soil wetness threshold and zone threshold are explored, where soil moisture threshold at 12 different exceedance probabilities are studied as well as 6 different values for the zone threshold.

3.4 Validation of thresholds for landslides

The evaluation of thresholds' prediction performance is based on contingency matrix, skill scores and the receiver operating characteristic (ROC) analysis, which are commonly used in assessment studies (Dai et al. 2015, Gariano, et al. 2015). For integrated thresholds, it should be noted that the contingency matrix is calculated based on rainfall events instead of calendar days. The reasons are as follows: 1) calculating contingencies based on calendar days can lead to an overestimation of false positives, because during one rainfall event, the soil wetness may exceed the threshold more than one day; however, in most cases, one landslide event is associated with one rainfall event at the same location; 2) This choice can facilitate our direct comparison with rainfall thresholds.

The contingency matrix consists of four components, as listed in Table 3. If thresholds predict landslide occurrences, it is Positive (P), otherwise, it is Negative (N). If the prediction is correct, it is True (T), on the contrary, it is False (F). Therefore, true positive (TP) means the threshold predicts landslide occurrences successfully; similarly, true negative (TN) means the threshold correctly predicts the non-occurrence of landslides. For false positive (FP), also known as false alarm, it is an error where the threshold predicts the occurrence of landslides; however, there are no landslide occurrences in reality. False negative (FN) is an error in which thresholds indicate the non-occurrences of landslides; however, in reality landslides occur, which is also known as missed alarm. With the contingency matrix, four skill scores are calculated to evaluate the prediction performance of thresholds.

Table 3 The Contingency Matrix

Predicted \ Observed	Yes	No
Yes	TP	FP
No	FN	TN

Hit Rate (HR), which is the proportion of the rainfall events that are predicted correctly to trigger landslides over all rainfall events that have triggered landslides, ranging between 0 and 1, with the optimal value as 1. It can be calculated as:

$$\mathrm{HR} = \frac{\mathrm{TP}}{\mathrm{TP} + \mathrm{FN}} \tag{2}$$

False Alarm Rate (FAR), which is the proportion of false alarms over the rainfall events that haven't triggered landslides, ranging between 0 and 1, with the optimal value as 0. It can be calculated as:

$$\mathrm{FAR} = \frac{\mathrm{FP}}{\mathrm{FP} + \mathrm{TN}} \tag{3}$$

Hanssen and Kuipers skill score (HK) (Hanssen and Kuipers 1965), which measures the prediction accuracy for the rainfall events with and without landslides, ranging between -1 and 1, with the optimal value as 1. It can be calculated as:

$$\mathrm{HK} = \mathrm{HR} - \mathrm{FAR} \tag{4}$$

The optimal prediction is achieved with HR as 1 and FAR as 0 (perfect point). Euclidean distance (d) between the prefect point and the prediction result could measure the prediction performance. The closer the prediction result to the perfect point, the better the prediction performance. Euclidean distance (d) can be calculated as:

$$\mathrm{d} = \sqrt{(\mathrm{HR} - 1)^2 + \mathrm{FAR}^2} \tag{5}$$

The overall predictive capability of a threshold scheme can be evaluated with the receiver operating characteristic (ROC) curve, with HR against FAR (Fawcett 2006). The area under the ROC curve (AUC) can be used as the criterion. The larger the AUC, the better the predictive capability.

4 Results

4.1 Rainfall thresholds for landslide occurrences

Figure 4 shows the distribution of rainfall conditions (D, E) that are likely to trigger landslides in the study area, over the period 2005-2013 (purple dots). Five regional thresholds with different exceedance probabilities are also shown. Rainfall conditions that are likely to result in landslides in the study area are in the range of duration $1\ day \leq D \leq 46\ days$, and in the range of cumulated event rainfall $5.2mm \leq E \leq 747.6mm$, which are the ranges of validity for the threshold. Taking the exceedance probability of 5% as an example, as expected, 10 pairs of the (D, E) data (5% of 212 rainfall conditions) below T_5 threshold. For the threshold at 50% exceedance probability, about half of the data are below T_{50} threshold. The uncertainties associated with thresholds depend on the number and distribution of the empirical data, which can be reduced with the increase of the data used to determine the thresholds.

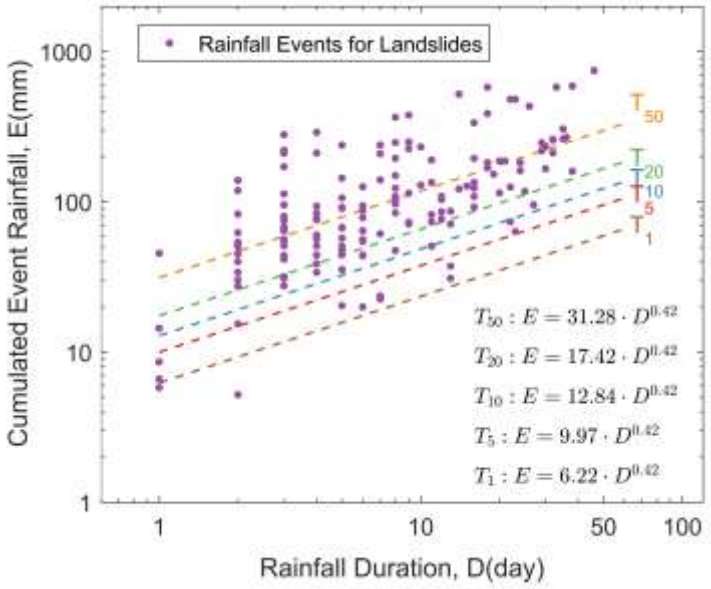

Figure 4. Rainfall duration D (x-axis) vs. cumulated event rainfall E (y-axis) conditions that are likely to trigger landslides over the calibration period 2005 to 2013 and the corresponding thresholds.

4.2 Soil Wetness Index (SWI)

The hydrological model is calibrated with the flow data for the period 2004-2013, with the first year as the warm-up period. The NSEs are 0.82 and 0.80 for Catchment 1 and Catchment 2 respectively. The model is then validated using the data from 2014 to 2015, the NSE value is 0.76 for both catchments. The calibrated model is regarded as acceptable to simulate the hydrological response to meteorological inputs, including the soil wetness condition's response. Due to the lack of in-situ soil wetness measurements in the study area, the soil wetness index estimated by the model cannot be calibrated. However, the hydrological model SHETRAN's capability to simulate the variation of soil water has been proved with measured data in the work of Birkinshaw (2008). It should be noted that the soil wetness index derived from the hydrological model is only considered as a proxy of soil water content because of the simplification of the model setting. The top soil depth is calibrated as 0.28m for both catchments. Therefore, the derived soil wetness index is the indication of the soil moisture condition of the shallow soil depth. The superiority of the derived soil wetness index is that it could account for the hydrological process that is controlled by meteorological conditions and topographic properties, which is not available for indexes that are derived from rainfall conditions without considering the hydrological process.

Taking the simulation results of year 2008 for Catchment 1 as an example, the characteristics of the derived soil wetness index are introduced. Figure 5 shows the time series of runoff simulations and the spatial distribution of soil wetness index. Here three representative periods are selected for analysis, as listed in Table 4. Period 1 is the representative of dry periods. Period 2 is for the periods with intense rainfall; however, its antecedent periods are relatively dry. As for Period 3, it has not only the intense rainfall but also wet antecedent periods. The rainfall data used here is the average value of all the weather stations, and the soil wetness index in Figure 5c is the last day value of the rainfall periods. As it can be seen from Figure 5b, the simulated runoff is generally in line with the observed except for the underestimation of some peak flows. The underestimation of peak flows is also the reason for the low value of NSE, because NSE is sensitive to high flow events. From Figure 5c, it is clear that the soil wetness condition is highly related to rainfall conditions, not only the current condition but also the antecedent condition. This is distinct for the comparison of soil wetness between Period 2 and Period 3. The rainfall intensity for Period 2 is 16.6 mm/day, higher than that of Period 3 (10.43 mm/day). However, due to the contribution of the antecedent rainfall preceding Period 3, its soil wetness index is higher than that of Period 2. In addition, the soil wetness index has a similar pattern in terms of spatial distribution. The grid cells near to the river are wetter than others, which could be explained by the topography, because in areas of the catchment where both hillslope profile and plan are concave, the soil will tend to be very wet, like the hillslope hollows and low-gradient slopes (Burt and Butcher 1985).

Table 4 The Rainfall Information for the Three Representative Periods

Period	Start Date	End Date	Duration (Day)	Cumulated rainfall (mm)
1	2008-07-12	2008-07-12	0	0
2	2008-05-18	2008-05-22	5	83
3	2008-12-10	2008-12-16	7	73

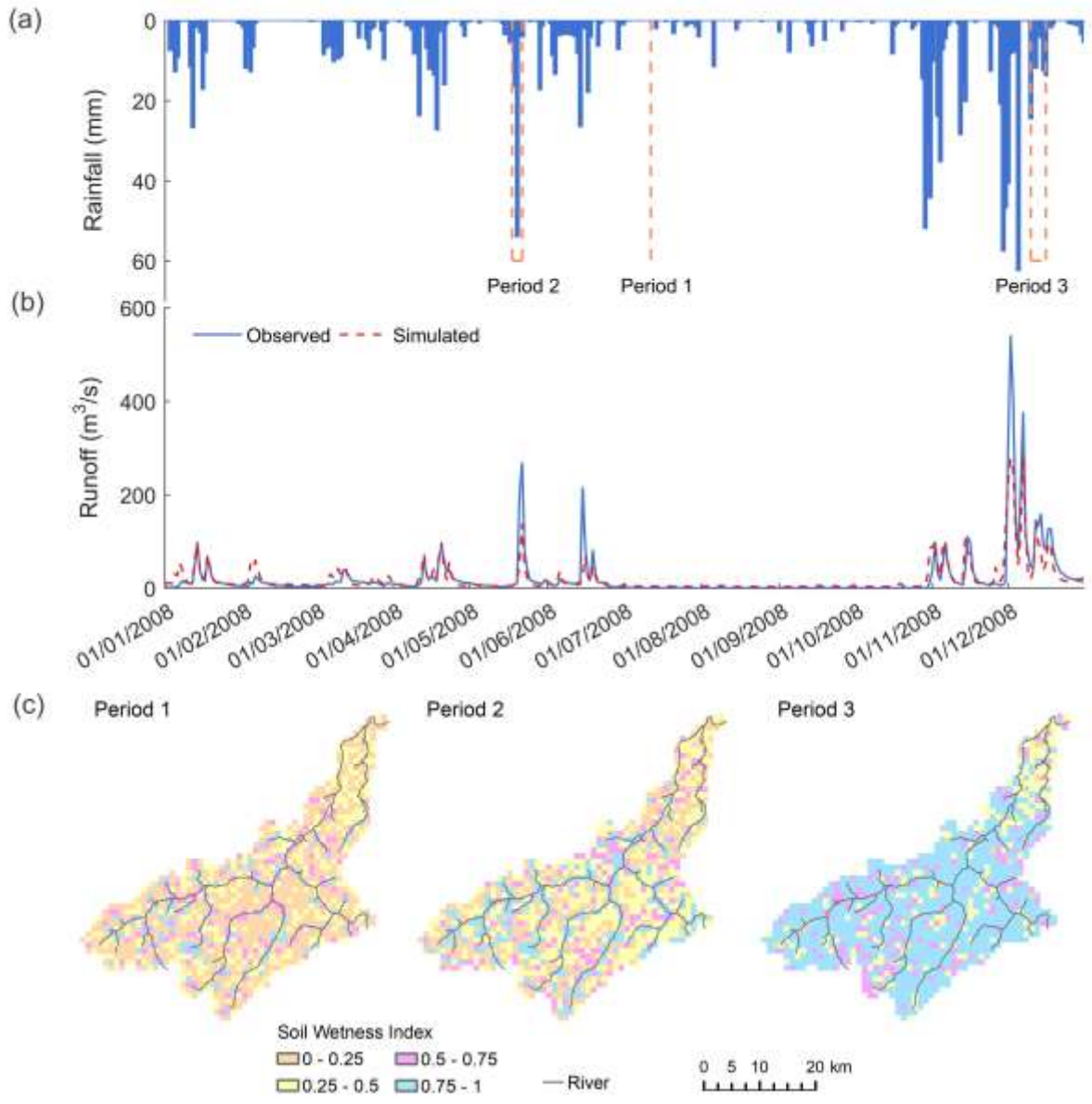

Figure 5. The results of model simulations for the year of 2008, a) the rainfall series as well as three representative periods; b) the comparison between observed runoff and simulated runoff; c) the spatial distribution of soil wetness index for three representative periods.

The temporal evolution of soil wetness index relies on the change of meteorological conditions, especially rainfall conditions. Therefore, we calculated the Pearson correlation coefficient (R) between soil wetness index and antecedent cumulated rainfall for each grid cell. Here different durations of the antecedent period are considered, including 3, 7, 15, 30, 60, 90, 120 and 150 days, referred as P_3, P_5, P_7, P_{15}, P_{30}, P_{60}, P_{90} and P_{120}, respectively. The distribution of correlation coefficients is shown with boxplots in Figure 6. It is seen that the soil wetness index has the best correlation relationship with P_{60} compared with other antecedent cumulated rainfall, whose median value is 0.73. As is expected, this value is not very high, because the soil wetness index is not only related to the antecedent rainfall but also the evapotranspiration and drainage, but the antecedent cumulated rainfall only considers the rainfall. The correlation coefficient for all antecedent periods has high variations for different grid cells. As only the spatial variation of DEM is considered in model simulations, this variation is attributed to the topographic properties.

In order to further explore the temporal evolution of soil wetness index, we selected three representative grid cells for analysis. These three grid cells belong to one alert zone and have the same meteorological conditions, whose locations and basic information are shown in Figure 7a. Grid Cell 1 is near to the river, Grid Cell 2 is at the foot of the hillslope, and Grid Cell 3 is on the hillside. We also calculated the topographic wetness index, TWI ($\ln(\alpha/\tan\beta)$), to infer topographic control on hydrological processes, where α is the local upslope area draining through a certain point and $\tan\beta$ is the local slope (BEVEN and Kirkby 1979). TWI could quantify the tendency of soil water distribution, which is affected by topography. The larger the value of TWI, the wetter the location. The value of TWI is 12.1 for Grid Cell 1, 9.28 for Grid Cell 2 and 8.58 for Grid Cell 3. Figure 7b shows the cumulated rainfall of the antecedent 60 days, which has better correlation relationship with the soil wetness index compared with other antecedent periods. Figure 7c presents the temporal evolution of soil wetness index for three representative grid cells. The time range for Figure 7b and Figure 7c is from 2008 to 2013, the reason for this choice is that most landslides occurred during this period. It is clear that the evolution of soil wetness index is in line with that of the antecedent cumulated rainfall for all the three grid cells. However, there are differences in terms of the variation range and the value of soil wetness index. For instance, it is easy for Grid Cell 1 to reach the wettest condition even the antecedent cumulated rainfall is not very large. However, for Grid Cell 2 and Grid Cell 3, only when the antecedent cumulated rainfall is high enough, the soil wetness index could reach the largest value 1. According to the value of TWI, it is expected that for the same rainfall conditions, Grid Cell 1 has wetter conditions than other grid cells, because the wetness condition of Grid Cell 1 is not only attributed by rainfall but also by some lateral flows. Based on the above, we could infer that the derived soil wetness index could reflect the hydrological process that is controlled by meteorological conditions and topographic properties.

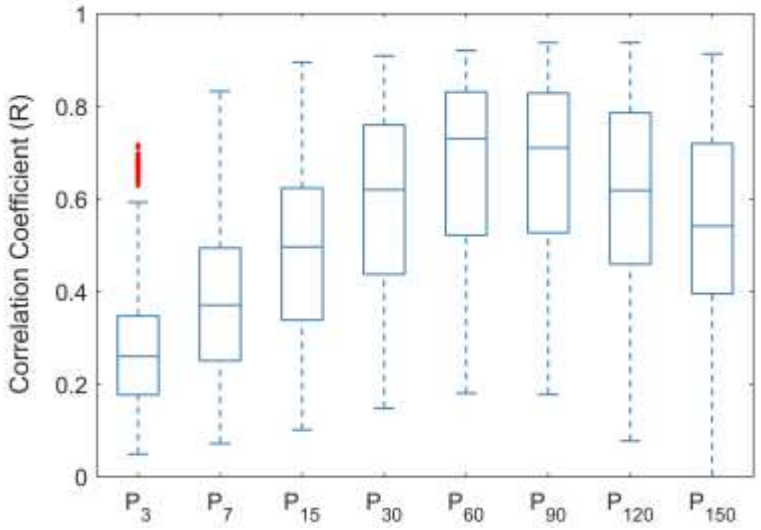

Figure 6. The boxplot of the correlation coefficient between soil wetness index and antecedent cumulated rainfall for all grid cells (P_i means the cumulated rainfall of the antecedent i days).

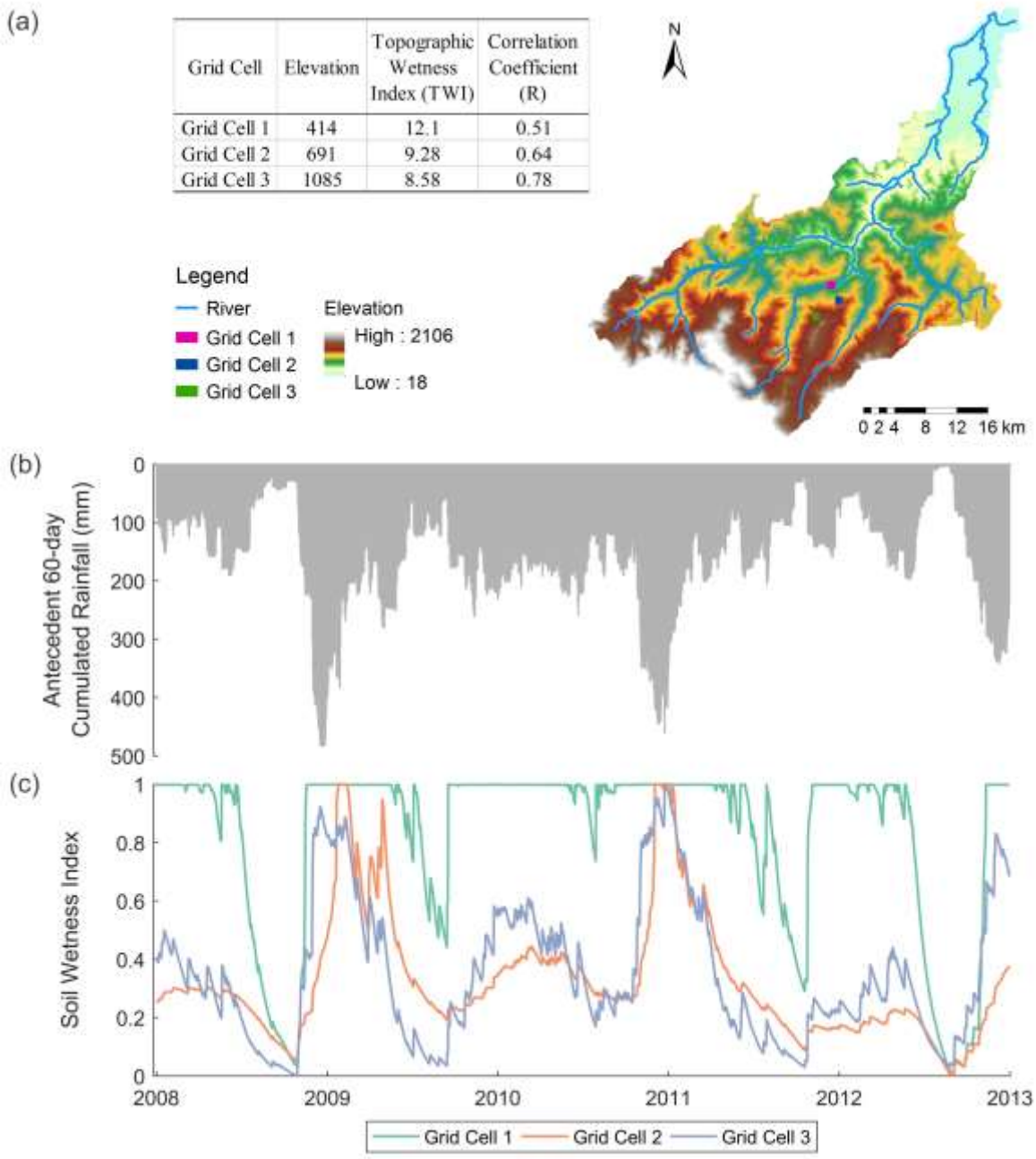

Figure 7. a) The location of three representative grid cells; b) the temporal evolution of cumulated rainfall of antecedent 60 days; c) the temporal evolution of soil wetness index for three grid cells.

4.3 Integrated landslide thresholds

The soil wetness threshold is determined by analyzing the soil wetness index of the landslides during the period 2005-2013, whose distribution is shown in Figure 8. The soil wetness index that is related to landslide occurrences ranges from 0.09 to 1. Despite there are some

landslides with a lower value in terms of soil wetness index, it is seen that about 90% of landslides have a soil wetness index higher than 0.6. In order to exclude the effect of some outlier cases (like landslides with relatively dry soil conditions), we determined the threshold value considering different exceedance probabilities. The percentiles of landslides' soil wetness index are used to determine the threshold values, as marked with triangles in Figure 8. The percentile rank considered in this study includes 1, 2, 3, 4, 5, 6, 7, 8, 9, 10, 20 and 50. Taking the threshold value determined by 10^{th} percentile (T_{10}) as an example, it means there are 10% landslides with a soil wetness index smaller than T_{10}.

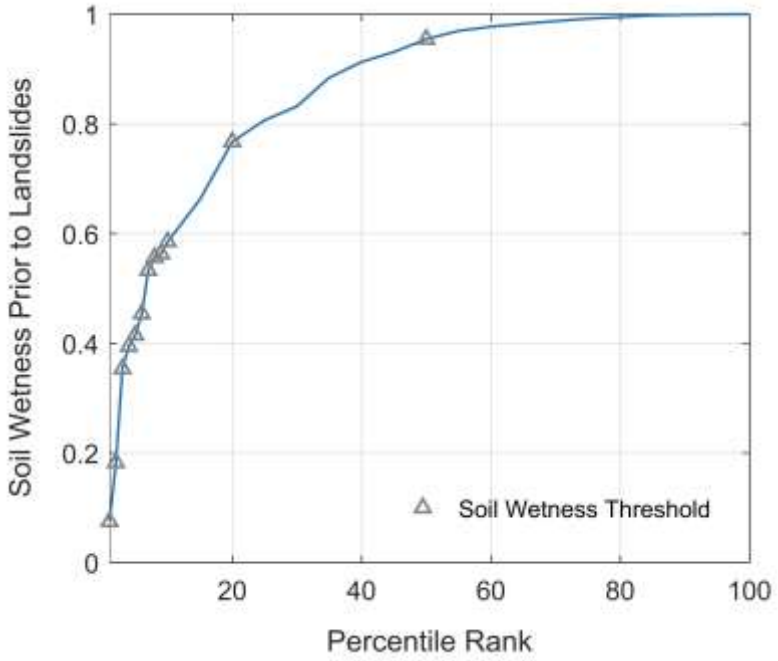

Figure 8. a) The distribution of soil wetness index value that is related to landslide occurrences, as well as threshold values determined using different percentiles.

The combination of soil wetness threshold and zone threshold constitute the integrated threshold for landslide occurrences. With 12 different soil wetness threshold values, 6 different zone thresholds (50%, 60%, 70%, 80%, 90% and 95%) are explored. The area under ROC curves (AUC) is used as the evaluation criterion to determine the optimal zone threshold value. This procedure is based on the data during the validation period 2014-2015. There are 817 rainfall events and 22 of them identified for landslide occurrences. The prediction results are shown in Figure 9. For the same curve, the zone threshold value remains the same, and the dots on each curve represents the variation of the soil wetness threshold value. Therefore, the area under the ROC curve (AUC) could quantify the performance of the zone threshold. The value of AUC increases as the zone threshold increases from 50% to 90%, and then decreases when the threshold is up to 95%. Since the zone threshold of 90% exhibits the optimal results, with a maximum value of AUC, we defined the zone threshold as 90% for the integrated thresholds.

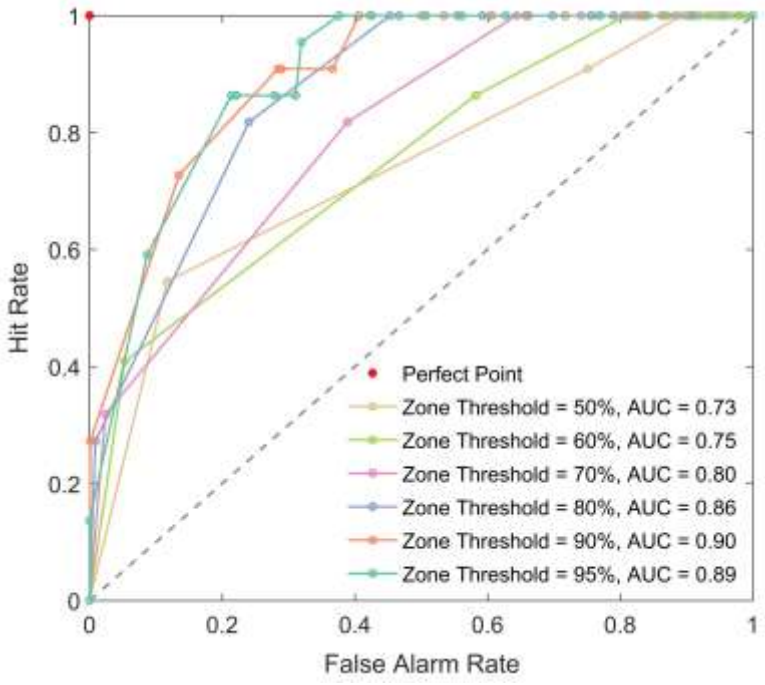

Figure 9. ROC curves for different zone thresholds in combination with soil wetness thresholds at 12 different exceedance probabilities.

4.4 Prediction performance of landslide thresholds

It is of great importance to evaluate the prediction performance of thresholds, in terms of increasing the number of correct predictions and reducing the number of incorrect predictions. We evaluate the predictive capability of the proposed integrated thresholds using contingencies, skill scores and ROC curves, with the data of the validation period. There are 817 rainfall events reconstructed for 16 rain gauges and 22 identified for 39 landslides during this period.

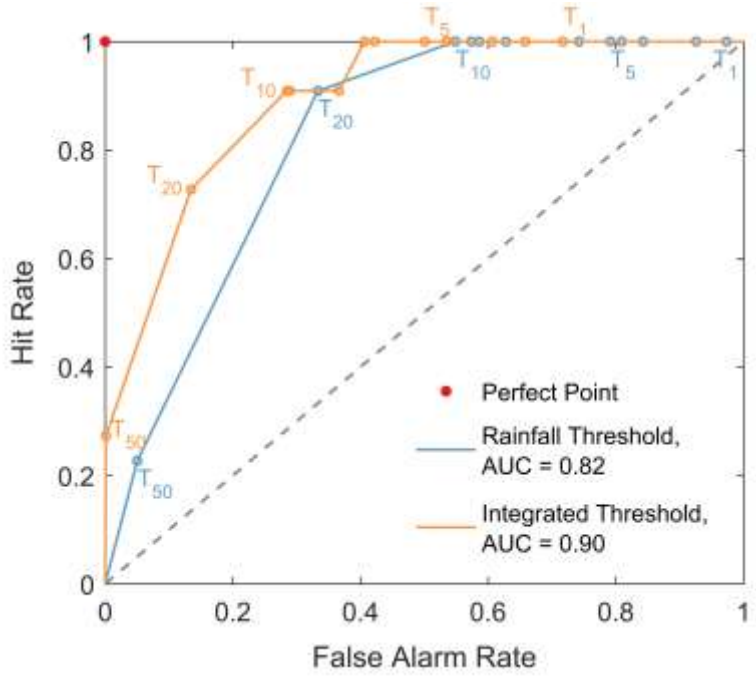

Figure 10. ROC curves for rainfall threshold and integrated threshold (with zone threshold of 90%).

The prediction performance of the integrated threshold is compared with that of the rainfall threshold for different exceedance probabilities. Their ROC curves are plotted in Figure 10. The AUC for rainfall threshold and integrated threshold is 0.82 and 0.90 respectively, indicating the integrated threshold (with zone threshold of 90%) has a better predictive capability than the rainfall threshold, regardless of the exceedance probability.

Table 5 lists four contingencies (TP, FP, FN and TN), as well as four skill scores (HR, FAR, HK and d) of thresholds at different probabilities. For both rainfall thresholds and integrated thresholds, with the increase of the exceedance probability, the performance in terms of FAR becomes better sometimes at the expense of reducing HR. There is an optimal balance between correct predictions and incorrect predictions. Considering the values of HK and d, the optimal result is observed at the maximum HK and minimum d, for rainfall thresholds, the optimal result reaches at the exceedance probability of 20%, whose HR is 0.909 and FAR is 0.333. As for the integrated threshold, the optimal result is obtained at the exceedance probability of 10%, with HR as 0.909 and FAR as 0.284. However, the optimal thresholds defined by the value of HK and d miss 2 landslides among 22 landslides. Due to the danger of missed alarms, a high HR is preferable if the threshold is used in an operational landslide early warning system. In this context, requiring the HR as 1, the rainfall threshold has the best performance at the exceedance probability of 10% with FAR as 0.548, as for the integrated threshold, its best result is obtained with the exceedance probability of 7% with FAR as 0.406. It is found for optimal thresholds determined by two

methods, the integrated threshold shows a better performance in terms of false alarm rate, compared with that of the rainfall threshold.

Table 5 Contingencies (TP, FP, FN, TN) and Skill Scores (HR, FAR, HK, d) for landslide thresholds at different exceedance probabilities (P) (the optimal thresholds are highlighted)

a) Rainfall thresholds

P (%)	TP	FN	FP	TN	HR	FAR	HK	d
1	22	0	774	21	1.000	0.974	0.026	0.974
2	22	0	736	59	1.000	0.926	0.074	0.926
3	22	0	670	125	1.000	0.843	0.157	0.843
4	22	0	643	152	1.000	0.809	0.191	0.809
5	22	0	629	166	1.000	0.791	0.209	0.791
6	22	0	590	205	1.000	0.742	0.258	0.742
7	22	0	499	296	1.000	0.628	0.372	0.628
8	22	0	466	329	1.000	0.586	0.414	0.586
9	22	0	456	339	1.000	0.574	0.426	0.574
10	22	0	436	359	**1.000**	**0.548**	**0.452**	**0.548**
20	20	2	265	530	**0.909**	**0.333**	**0.576**	**0.346**
50	5	17	40	755	0.227	0.050	0.177	0.774

b) Integrated thresholds (with the zone threshold of 90%)

P (%)	TP	FN	FP	TN	HR	FAR	HK	d
1	22	0	570	225	1.000	0.717	0.283	0.717
2	22	0	523	272	1.000	0.658	0.342	0.658
3	22	0	482	313	1.000	0.606	0.394	0.606
4	22	0	425	370	1.000	0.535	0.465	0.535
5	22	0	398	397	1.000	0.501	0.499	0.501
6	22	0	336	459	1.000	0.423	0.577	0.423
7	22	0	323	472	**1.000**	**0.406**	**0.594**	**0.406**
8	20	2	291	504	0.909	0.366	0.543	0.377
9	20	2	230	565	0.909	0.289	0.620	0.303
10	20	2	226	569	**0.909**	**0.284**	**0.625**	**0.298**
20	16	6	107	688	0.727	0.135	0.593	0.304
50	6	16	1	794	0.273	0.001	0.271	0.727

5 Discussion

The importance of soil moisture conditions on landslide occurrence has been highly recognized and discussed (Bogaard and Greco 2016, Collins and Znidarcic 2004, Ponziani et al. 2012). However, due to the scarcity of soil moisture data and the better available of rainfall data, rainfall information is mostly used in the published literature. There are several limitations in using rainfall characteristics (e.g. rainfall duration, rainfall intensity, cumulated event rainfall and antecedent rainfall) to predict landslides. First, for most studies, the identification of rainfall events

and rainfall conditions responsible for landslides is subjective. Only a few researches highlight the importance of the objective criteria to detect rainfall events with landslides and measure their characteristics (Berti, et al. 2012, Melillo, et al. 2014). The lack of objective criteria may bring uncertainties to the definition of rainfall thresholds, limiting their use in the operational warning systems. Second, it is of great importance to take antecedent soil moisture conditions into account. Even some investigators used the antecedent rainfall conditions as a proxy, it is difficult to identify how long the antecedent period should be. As for the soil moisture, their temporal evolution is responsive to the changes of rainfall conditions, and the value is a result of multiple factors, like the conditions of current rainfall, antecedent rainfall, evapotranspiration and topography. Therefore, soil moisture data especially the distributed ones are able to provide more vital information for the initiation of landslides. This study explores the application of distributed hydrological simulations in landslide predictions by using it to derive the distributed soil wetness index. The derived soil wetness index is capable of reflecting the hydrological process that is controlled by meteorological conditions and topographic properties. The soil wetness index is then used to define integrated thresholds for landslide occurrences. The better performance of the integrated thresholds over the rainfall thresholds demonstrates the effectiveness of using the derived soil wetness index in landslide predictions. Besides, the proposed integrated threshold provides a new perspective to make use of the high-resolution information in zone-based landslide predictions. Despite these facts, there are several limitations worth noting.

We derived the soil wetness index using the distributed hydrological model. Due to the lack of the measured soil moisture data, the derived soil wetness index is not able to be validated, which is a limitation of this study. However, a detailed plausibility check has been carried out. The hydrological model that is calibrated with the measured flow is commonly considered capable of simulating hydrological processes, including the variation of the soil water content. Therefore, we think the soil wetness index derived from the well-calibrated model could reflect the hydrological process, which is superior to indexes that are derived from rainfall conditions without considering the hydrological process. In addition, through analyzing the spatial distribution of soil wetness index, it proves in line with the physical process. The temporal evolution of soil wetness index also has a good correlation relationship with the meteorological conditions. Therefore, in spite of the lack of validation in terms of soil wetness index, the index is considered effective to indicate the soil moisture conditions. It should be noted that the hydrological simulations in this study rely on the spatially uniform parameters, so the simulated soil water content is only regarded as an index of the soil moisture condition. However, if the distributed model takes into account the spatial variation of land cover and soil type when the required information is available, the simulated soil water content is considered capable of reflecting the real soil water content, which will be explored in the future work.

When applying the soil wetness index in landslide predictions, the threshold is only based on one variable: soil wetness index, which may affect the threshold's prediction performance. In general, the initiation of rainfall-induced landslides is attributed to the antecedent factors that predispose hillslope to failure (like soil moisture conditions) and the recent trigger factors (like the recent rainfall events), as a result, the hydro-meteorological thresholds is popular to consider both the antecedent soil moisture conditions and the recent rainfall conditions (Bogaard and Greco 2018, Chleborad et al. 2008, Mirus et al. 2018, Mirus, et al. 2018). In this study, we used the soil wetness index to characterize these two types of information, because the soil wetness index on the day of landslide occurrences could account for both antecedent soil wetness conditions and recent rainfall conditions. It is found that separately considering the antecedent wetness condition and the recent rainfall in the threshold definition could benefit the threshold's prediction performance, compared with integrating these two types of information into one variable (Zhao, et al. 2019). Therefore, we think the prediction performance will be improved if the proposed soil wetness index is used to characterize the antecedent soil moisture condition, which is then combined with the recent rainfall condition to determine the landslide thresholds. However, combining the antecedent soil moisture condition and recent rainfall in threshold definition will raise many problems (like the determination of the antecedent period and the landslide definition method), which is beyond the scope of this study. Given the operability of thresholds in landslide predictions, the prediction procedure is carried out based on alert zones. In order to connect the grid-based soil wetness index to the alert zone, a zone threshold is introduced to help evaluate the proportion of the wet grid cells, where the wet grid cell is evaluated by the soil wetness threshold. The combination of the soil wetness threshold and the zone threshold constitute the integrated threshold, provides a way to make use of the high-resolution data in the landslide prediction that is based on alert zones.

The evaluation of landslide threshold is based on the compromise between increasing correct predictions and reducing incorrect predictions, without considering additional weighting factors. However, in the operational landslide early warning systems, weightings should be considered, because the cost of missed alarms and false alarms are affected by multiple factors. For example, for the region where the cost of missed alarms is much higher than that of false alarms, a larger weight should be given to missed alarms or HR, otherwise, the importance of false alarms should be highlighted. Besides, the damage caused by landslides also depends on the exposure of the population to the region, which varies with times. For instance, there are larger populations in a sightseeing attraction during holidays compared with weekdays. Therefore, the definition of landslide thresholds should be carried out dynamically by evaluating the landslide risk.

6 Conclusion

In this study, we derived a soil wetness index using the distributed hydrological model and then applied it to landslide predictions. The derived soil wetness index could account for the hydrological process that is controlled by meteorological conditions and topographic properties, superior to indexes that are derived from rainfall conditions without considering the hydrological process. The soil wetness index is used to determine soil wetness threshold for landslide occurrences, which is combined with a zone threshold to predict landslides for an alert zone, referred as the integrated threshold. The integrated threshold provides a perspective to connect high-resolution data to the alert zone, benefiting the application of high-resolution data in operational landslide early warning systems. The prediction performance of the integrated threshold is evaluated with the use of skill scores and receiver operating characteristic (ROC) curves. Results show that the integrated threshold has a better predictive capability than the rainfall threshold, especially in reducing false alarms. The better performance of the integrated threshold demonstrates the effectiveness of using the derived soil wetness index in landslide predictions.

Our results reported here further highlight the potential of applying hydrological simulations in landslide prediction studies. Although this study is carried out in two catchments in the Emilia-Romagna region, we hypothesize that the proposed methods are applicable to other areas with sufficient data. Therefore, more explorations of the proposed methods are encouraged in order to support or falsify this hypothesis.

References

Abbott M, Bathurst J, Cunge J, O'connell P and Rasmussen J (1986) An introduction to the european hydrological system—systeme hydrologique europeen,"she", 2: Structure of a physically-based, distributed modelling system. Journal of hydrology 87: 61-77.

Baum RL and Godt JW (2009) Early warning of rainfall-induced shallow landslides and debris flows in the USA. Landslides 7: 259-272. doi: 10.1007/s10346-009-0177-0

Berti M, Martina MLV, Franceschini S, Pignone S, Simoni A and Pizziolo M (2012) Probabilistic rainfall thresholds for landslide occurrence using a bayesian approach. Journal of Geophysical Research: Earth Surface 117. doi: 10.1029/2012jf002367

Bertolini G and Pellegrini M (2001) The landslides of the emilia apennines (northern italy) with reference to those which resumed activity in the 1994–1999 period and required civil protection interventions. Quad Geol Appl 8: 27-74.

Bettelli G and Vannucchi P (2003) Structural style of the offscraped ligurian oceanic sequences of the northern apennines: New hypothesis concerning the development of mélange block-in-matrix fabric. Journal of Structural Geology 25: 371-388.

BEVEN KJ and Kirkby MJ (1979) A physically based, variable contributing area model of basin hydrology/un modèle à base physique de zone d'appel variable de l'hydrologie du bassin versant. Hydrological Sciences Journal 24: 43-69.
Birkinshaw SJ (2008) Physically-based modelling of double-peak discharge responses at slapton wood catchment. Hydrological Processes 22: 1419-1430. doi: 10.1002/hyp.6694
Birkinshaw SJ and Ewen J (2000) Nitrogen transformation component for shetran catchment nitrate transport modelling. Journal of hydrology 230: 1-17.
Bogaard T and Greco R (2018) Invited perspectives: Hydrological perspectives on precipitation intensity-duration thresholds for landslide initiation: Proposing hydro-meteorological thresholds. Natural Hazards and Earth System Sciences 18: 31-39. doi: 10.5194/nhess-18-31-2018
Bogaard TA and Greco R (2016) Landslide hydrology: From hydrology to pore pressure. Wiley Interdisciplinary Reviews: Water 3: 439-459.
Brocca L, Melone F and Moramarco T (2008) On the estimation of antecedent wetness conditions in rainfall–runoff modelling. Hydrological Processes 22: 629-642.
Brocca L, Ponziani F, Moramarco T, Melone F, Berni N and Wagner W (2012) Improving landslide forecasting using ascat-derived soil moisture data: A case study of the torgiovannetto landslide in central italy. Remote Sensing 4: 1232-1244. doi: 10.3390/rs4051232
Brunetti M, Peruccacci S, Rossi M, Luciani S, Valigi D and Guzzetti F (2010) Rainfall thresholds for the possible occurrence of landslides in italy. Natural Hazards and Earth System Sciences 10: 447-458.
Burt T and Butcher D (1985) Topographic controls of soil moisture distributions. Journal of Soil Science 36: 469-486.
Calvello M, d'Orsi RN, Piciullo L, Paes N, Magalhaes M and Lacerda WA (2015) The rio de janeiro early warning system for rainfall-induced landslides: Analysis of performance for the years 2010–2013. International Journal of Disaster Risk Reduction 12: 3-15. doi: 10.1016/j.ijdrr.2014.10.005
Campbell RH (1975) Soil slips, debris flows, and rainstorms in the santa monica mountains and vicinity, southern california. US Geological Survey, Professional Paper 851: 51.
Cardinali M, Galli M, Guzzetti F, Ardizzone F, Reichenbach P and Bartoccini P (2006) Rainfall induced landslides in december 2004 in south-western umbria, central italy: Types, extent, damage and risk assessment. Natural Hazards and Earth System Science 6: 237-260.
Chleborad AF, Baum RL, Godt JW and Powers PS (2008) A prototype system for forecasting landslides in the seattle, washington, area. Reviews in Engineering Geology 20: 103-120. doi: 10.1130/2008.4020(06)
Collins BD and Znidarcic D (2004) Stability analyses of rainfall induced landslides. Journal of geotechnical and geoenvironmental engineering 130: 362-372.

Croley II TE and Hartmann HC (1985) Resolving thiessen polygons. Journal of Hydrology 76: 363-379.

Crozier MJ (1999) Prediction of rainfall ‐ triggered landslides: A test of the antecedent water status model. Earth surface processes and landforms 24: 825-833.

Dahal RK and Hasegawa S (2008) Representative rainfall thresholds for landslides in the nepal himalaya. Geomorphology 100: 429-443. doi: 10.1016/j.geomorph.2008.01.014

Dai Q, Rico-Ramirez MA, Han D, Islam T and Liguori S (2015) Probabilistic radar rainfall nowcasts using empirical and theoretical uncertainty models. Hydrological Processes 29: 66-79. doi: 10.1002/hyp.10133

Ewen J (1995) Contaminant transport component of the catchment modelling system shetran. Wiley, Chichester, UK,

Fawcett T (2006) An introduction to roc analysis. Pattern recognition letters 27: 861-874.

Gariano SL, Brunetti MT, Iovine G, Melillo M, Peruccacci S, Terranova O, Vennari C and Guzzetti F (2015) Calibration and validation of rainfall thresholds for shallow landslide forecasting in sicily, southern italy. Geomorphology 228: 653-665. doi: 10.1016/j.geomorph.2014.10.019

Glade T, Crozier M and Smith P (2000) Applying probability determination to refine landslide-triggering rainfall thresholds using an empirical “antecedent daily rainfall model”. Pure and Applied Geophysics 157: 1059-1079.

Greco R, Guida A, Damiano E and Olivares L (2010) Soil water content and suction monitoring in model slopes for shallow flowslides early warning applications. Physics and Chemistry of the Earth, Parts A/B/C 35: 127-136. doi: 10.1016/j.pce.2009.12.003

Guzzetti F, Peruccacci S, Rossi M and Stark CP (2007) The rainfall intensity–duration control of shallow landslides and debris flows: An update. Landslides 5: 3-17. doi: 10.1007/s10346-007-0112-1

Guzzetti F, Peruccacci S, Rossi M and Stark CP (2007) Rainfall thresholds for the initiation of landslides in central and southern europe. Meteorology and Atmospheric Physics 98: 239-267. doi: 10.1007/s00703-007-0262-7

Hanssen A and Kuipers W (1965) On the relationship between the frequency of rain and various meteorological parameters:(with reference to the problem ob objective forecasting). Staatsdrukkerij-en Uitgeverijbedrijf,

Hawke R and McConchie J (2011) In situ measurement of soil moisture and pore-water pressures in an 'incipient' landslide: Lake tutira, new zealand. J Environ Manage 92: 266-274. doi: 10.1016/j.jenvman.2009.05.035

Ibsen ML and Casagli N (2004) Rainfall patterns and related landslide incidence in the porretta-vergato region, italy. Landslides 1. doi: 10.1007/s10346-004-0018-0

Melillo M, Brunetti MT, Peruccacci S, Gariano SL and Guzzetti F (2014) An algorithm for the objective reconstruction of rainfall events responsible for landslides. Landslides 12: 311-320. doi: 10.1007/s10346-014-0471-3

Mirus B, Morphew M and Smith J (2018) Developing hydro-meteorological thresholds for shallow landslide initiation and early warning. Water 10. doi: 10.3390/w10091274

Mirus BB, Becker RE, Baum RL and Smith JB (2018) Integrating real-time subsurface hydrologic monitoring with empirical rainfall thresholds to improve landslide early warning. Landslides 15: 1909-1919. doi: 10.1007/s10346-018-0995-z

Nash JE and Sutcliffe JV (1970) River flow forecasting through conceptual models part i—a discussion of principles. Journal of hydrology 10: 282-290.

Norouzi Banis Y, Bathurst J and Walling D (2004) Use of caesium‐137 data to evaluate shetran simulated long‐term erosion patterns in arable lands. Hydrological processes 18: 1795-1809.

Parkin G (1996) A three-dimensional variably-saturated subsurface modelling system for river basins.

Peruccacci S, Brunetti MT, Gariano SL, Melillo M, Rossi M and Guzzetti F (2017) Rainfall thresholds for possible landslide occurrence in italy. Geomorphology 290: 39-57. doi: 10.1016/j.geomorph.2017.03.031

Peruccacci S, Brunetti MT, Luciani S, Vennari C and Guzzetti F (2012) Lithological and seasonal control on rainfall thresholds for the possible initiation of landslides in central italy. Geomorphology 139-140: 79-90. doi: 10.1016/j.geomorph.2011.10.005

Pini GA (1999) Tectonosomes and olistostromes in the argille scagliose of the northern apennines, italy. Geological Society of America,

Ponziani F, Pandolfo C, Stelluti M, Berni N, Brocca L and Moramarco T (2012) Assessment of rainfall thresholds and soil moisture modeling for operational hydrogeological risk prevention in the umbria region (central italy). Landslides 9: 229-237.

Posner AJ and Georgakakos KP (2015) Soil moisture and precipitation thresholds for real-time landslide prediction in el salvador. Landslides 12: 1179-1196. doi: 10.1007/s10346-015-0618-x

Ray RL, Jacobs JM and Cosh MH (2010) Landslide susceptibility mapping using downscaled amsr-e soil moisture: A case study from cleveland corral, california, us. Remote Sensing of Environment 114: 2624-2636. doi: 10.1016/j.rse.2010.05.033

Rossi M, Witt A, Guzzetti F, Malamud BD and Peruccacci S (2010) Analysis of historical landslide time series in the emilia-romagna region, northern italy. Earth Surface Processes and Landforms 35: 1123-1137. doi: 10.1002/esp.1858

Segoni S, Leoni L, Benedetti A, Catani F, Righini G, Falorni G, Gabellani S, Rudari R, Silvestro F and Rebora N (2009) Towards a definition of a real-time forecasting network for rainfall induced shallow landslides. Natural Hazards and Earth System Sciences 9: 2119-2133.

Temimi M, Leconte R, Chaouch N, Sukumal P, Khanbilvardi R and Brissette F (2010) A combination of remote sensing data and topographic attributes for the spatial and temporal monitoring of soil wetness. Journal of Hydrology 388: 28-40.

Vai GB, Vai F, Martini IP and Martini P (2001) Anatomy of an orogen: The apennines and adjacent mediterranean basins. Springer Science & Business Media,

Valenzuela P, Domínguez-Cuesta MJ, Mora García MA and Jiménez-Sánchez M (2017) Rainfall thresholds for the triggering of landslides considering previous soil moisture conditions (asturias, nw spain). Landslides 15: 273-282. doi: 10.1007/s10346-017-0878-8

Zêzere J, Vaz T, Pereira S, Oliveira S, Marques R and Garcia R (2015) Rainfall thresholds for landslide activity in portugal: A state of the art. Environmental Earth Sciences 73: 2917-2936.

Zêzere JL, Trigo RM and Trigo IF (2005) Shallow and deep landslides induced by rainfall in the lisbon region (portugal): Assessment of relationships with the north atlantic oscillation. Natural Hazards and Earth System Science 5: 331-344.

Zhang J and Han D (2017) Catchment morphing (cm): A novel approach for runoff modeling in ungauged catchments. Water Resources Research 53: 10899-10907.

Zhang R, Santos CA, Moreira M, Freire PK and Corte-Real J (2013) Automatic calibration of the shetran hydrological modelling system using msce. Water resources management 27: 4053-4068.

Zhao B, Dai Q, Han D, Dai H, Mao J and Zhuo L (2019) Antecedent wetness and rainfall information in landslide threshold definition. Hydrol Earth Syst Sci Discuss 2019: 1-26. doi: 10.5194/hess-2019-150

Zhao B, Dai Q, Han D, Dai H, Mao J and Zhuo L (2019) Probabilistic thresholds for landslides warning by integrating soil moisture conditions with rainfall thresholds. Journal of Hydrology.

Zhuo L, Dai Q, Han D, Chen N, Zhao B and Berti M (2019) Evaluation of remotely sensed soil moisture for landslide hazard assessment. IEEE Journal of Selected Topics in Applied Earth Observations and Remote Sensing 12: 162-173. doi: 10.1109/jstars.2018.2883361